P1.23 HISTOGRAM MATCHING OF ASMR-E AND TMI BRIGHTNESS TEMPERATURES

Thomas A. Jones* and Daniel J. Cecil
Department of Atmospheric Science
University of Alabama in Huntsville
Huntsville, AL

1. Introduction

A microwave-enhanced version of the Statistical Hurricane Intensity Prediction Scheme (SHIPS) is trained on a passive microwave sample consisting of Special Sensor Microwave Imager (SSM/I) and TRMM Microwave Imager (TMI) tropical cyclone overpasses utilizing 19.35, 37.0, and 85.5-GHz channels (Jones 2004, Jones et al. 2006). This new prediction scheme is referred to as SHIPS-MI. To increase sample size and real time data availability, Advanced Microwave Scanning Radiometer (ASMR-E) overpasses were applied to SHIPS-MI beginning in 2004. The ASMR-E instrument uses 18.4, 36.5, and 89.0-GHz channels in place of the 19.35, 37.0, and 85.5-GHz channels used by SSM/I and TMI. While the physical interpretation of these channels is the same across all sensors, brightness temperature (T_b) differences on the order of 10 K exist between AMSR-E and TMI over low precipitation regions. For example, the ocean surface emits slightly less microwave radiation at 18.4 vs. 19.35-GHz. As a result, 18.4-GHz T_b are colder than 19.35-GHz T_b for the same observation region. Thus, AMSR-E 18.4-GHz T_b are generally slightly cooler than their TMI counterparts while AMSR-E 89.0-GHz T_b are slightly warmer than TMI 85-GHz T_b.

In order to use AMSR-E data in a model trained from 19, 37, and 85-GHz data, the AMSR-E 18, 36, and 89-GHz T_b must be adjusted to simulate 19, 37, and 85-GHz T_b. Both horizontal (H) and vertical (V) polarizations for each channel are adjusted. An adjustment utilizing the difference in radiative properties between AMSR-E and TMI sensors is quite complex; thus, a simpler statistical approach is desired. A histogram-matching technique is used to match AMSR-E brightness temperatures to a baseline histogram derived from TMI brightness temperatures. Data from the TMI (and not SSM/I) are used as the adjustment standard since TMI has a similar spatial resolution as AMSR-E.

* *Corresponding author address*: Thomas A. Jones University of Alabama in Huntsville, 320 Sparkman Dr. Huntsville, AL 35805. email: tjones@nsstc.uah.edu

2. Data

The comparison histograms are computed from 10 TMI and AMSR-E 2004 tropical cyclone overpasses that occur within 2 h of each other. Each overpass is centered on the best track location of the tropical cyclone interpolated to the overpass time. Data out to a distance 300 km from the tropical cyclone center are considered. It is assumed that the overall microwave signature of a tropical cyclone remains relatively constant over a period of 2 h. The nature of AMSR-E and TMI orbits makes concurrent overpasses quite rare. The adjustment is trained on tropical cyclone overpasses rather than entire swaths in order to maximize adjustment accuracy for tropical cyclone observations.

3. Methodology

Histogram matching consists of matching the T_b histogram from one satellite sample (ASMR-E) to that of a reference sample (TMI) to calculate adjusted T_b (Richards and Jia 1999). The application of this technique requires the calculation of Cumulative Distribution Functions (CDFs) from the TMI and AMSR-E data. AMSR-E/TMI T_b pairs are selected along each CDF where cumulative probabilities are equal. A best-fit model between the paired data is created. The best-fit coefficients are then used to simulate 19, 37, and 85-GHz T_b from the AMSR-E 18, 36, and 89-GHz T_b.

Below approximately 250 K, AMSR-E 89-GHz and TMI 85-GHZ are essentially equal and do not require adjustment. Thus, the 89/85-GHz adjustment is only trained and applied to ASMR-E 89-GHz $T_b > 245$ K. Similarly the 36-GHz channel does not require adjustment for $T_b < 205$ K. Applying an adjustment beyond these limits would have the effect on increasing TMI/AMSR-E differences.

4. Results

The largest TMI/ASMR-E difference occurs for H19 and H18 channels between 140 and 180 K (Fig. 1a). TMI H19 is substantially warmer than H18 below 200 K. If H18 data were to be used in place of H19, forecast errors of several

knots would occur for tropical cyclones with below normal precipitation signatures. Differences between H36 and H37 are limited to less than 5 K while differences between 5 and 10 K exist between H85 and H89 (Figs. 2a, 3a). Data outside the 36 and 89-GHz adjustment thresholds are not included in the CDFs. Similar characteristics were observed for the vertical polarizations of these channels, though the magnitude of the T_b difference was somewhat less (not shown).

To adjust AMSR-E T_b to the TMI standard, T_b pairs along the CDF curves in Figures 1-3a are selected along lines of equal probability. For example, a cumulative probability of 0.2 in Fig. 1a produces the T_b pair 160 K (AMSR-E 18-GHz) and 175 K (TMI 19-GHz). Multiple T_b pairs are selected and plotted against each other in Figs. 1b, 2b, and 3b with a 1:1 reference line shown for comparison. Adjustment coefficients are derived from the T_b pairs under the assumption that a T_b pair containing TMI and adjusted AMSR-E data should match the 1:1 reference as close as possible. For each channel, best-fit lines are calculated from the T_b pairs using a single predictor linear regression analysis with units in degrees Kelvin (Eqs. 1-3). Each explains well over 99% of the variance present in the paired data. These equations are then applied to the AMSR-E data forming adjusted channels whose CDFs are also plotted in Figures 1-3a.

$$H19_{ADJ} = 31.3231 + 0.8814 \times H18_{AMSRE} \quad (1)$$
$$H37_{ADJ} = 4.0615 + 0.9745 \times H36_{AMSRE} \quad (2)$$
$$H85_{ADJ} = 23.0939 + 0.9018 \times H89_{AMSRE} \quad (3)$$

Overall, the adjusted CDFs closely match the TMI standard and eliminate much of the T_b difference between the two instruments. Equal probability TMI and adjusted AMSR-E T_b pairs lie much closer to the 1:1 reference than previously (Figs 1-3b). The adjustment accuracy decreases slightly as a function of increasing frequency. For 19 and 37-GHz adjustments, accuracy is within ±2 K of the TMI T_b (Figs. 1b and 2b) However, the relationship between AMSR-E H89 and TMI H85 appears to be non-linear between 250 and 260 K resulting in a somewhat larger error (Fig. 3b). This temperature range corresponds with the transition from scattering of 85-GHz radiation at lower T_b to emission at higher T_b. The non-linearity of differences between 85 and 89-GHz radiation can be dealt with by applying more complex fits to the T_b pairs in Figure 3b. Interestingly when H85 and V85 data are combined to form PCT85 data (Spencer et al. 1989), which is used in SHIPS-MI, the non-linearity of the adjustment between 250 and 260 K decreases.

Generally speaking, the accuracy of the adjustment is deemed good enough for use in an operational form of SHIPS-MI and possible future training samples. It is also expected to incorporate data from the next generation of SSM/I (SSMIS) into SHIPS-MI using this technique.

5. Example

H18, H36, and H89 data from an AMSR-E overpass of Hurricane Ivan at 1543 UTC 4 September 2004 are adjusted to the TMI standard using Equations 1-3 (Figs. 4-6). Shown for comparison are H19, H37, and H85 data from a TMI overpass at 1537 UTC. The largest difference between raw and adjusted T_b occurs when AMSR-E H18 is adjusted to H19 (Fig. 4a-b). Observe the large area of ~150 K H18 T_b present outside the inner core of Ivan on the non-adjusted overpass. The adjustment to H19 increases these T_b by ~15 K (Fig. 4b) resulting in a much better agreement with the concurrent TMI H19 T_b (Fig. 4c). The adjusted H19 160 K contour is an excellent match to the corresponding contour on the TMI overpass. The adjustment has little effect in higher precipitation regions as evidenced by similar placement of 200 K contours on both adjusted and non-adjusted data. Little noticeable difference exists between ASMR-E H36 and adjusted H37 T_b data (Fig. 5). Recall that no adjustment is made for H36 < 205 K. The differences, often less than 5 K, are difficult to visualize in this image. Still, agreement between the adjusted H37 and TMI H37 data is excellent. The adjustment is somewhat more apparent with AMSR-E H89 (Fig. 6). The areal coverage of H89 > 270 K decreases after adjustment to H85. The decrease more closely matches the areal coverage present in TMI H85 data. Given that the 89/85-GHz adjustment had the poorest fit, the adjustment still improves comparability between AMSR-E H89 and TMI H85 data by a significant margin.

Acknowledgements

Funding for this research was made possible by NASA grant NAG-512563. TMI and AMSR-E data provided by Goddard Space Flight Center. We would also like to acknowledge the staff of GHRC and the University of Alabama in Huntsville for their assistance in making this work possible.

References

Jones, T. A., 2004: Improving Hurricane Intensity Forecasting by Combining Microwave Imagery with the SHIPS model. Preprints, *26th Conference on Hurricanes and Tropical Meteorology*. 2-7 May, Amer. Meteor. Soc., Miami, Florida, **P1.51**. 346-7.

Jones, T. A., D. J. Cecil, and M. DeMaria, 2006: Passive Microwave-Enhanced Statistical Hurricane Intensity Prediction Scheme. *Wea. and Forecasting*. In review.

Richards and Jia, 1999: *Remote Sensing Digital Image Analysis, An Introduction*. Springer, 363 pp.

Spencer, R. W., H. M. Goodman, and R. E. Hood, 1989: Precipitation retrieval over land and ocean with SSM/I: Identification and characteristics of the scattering signal. *J. Atmos. Oceanic Technol.*, **6**, 254-273.

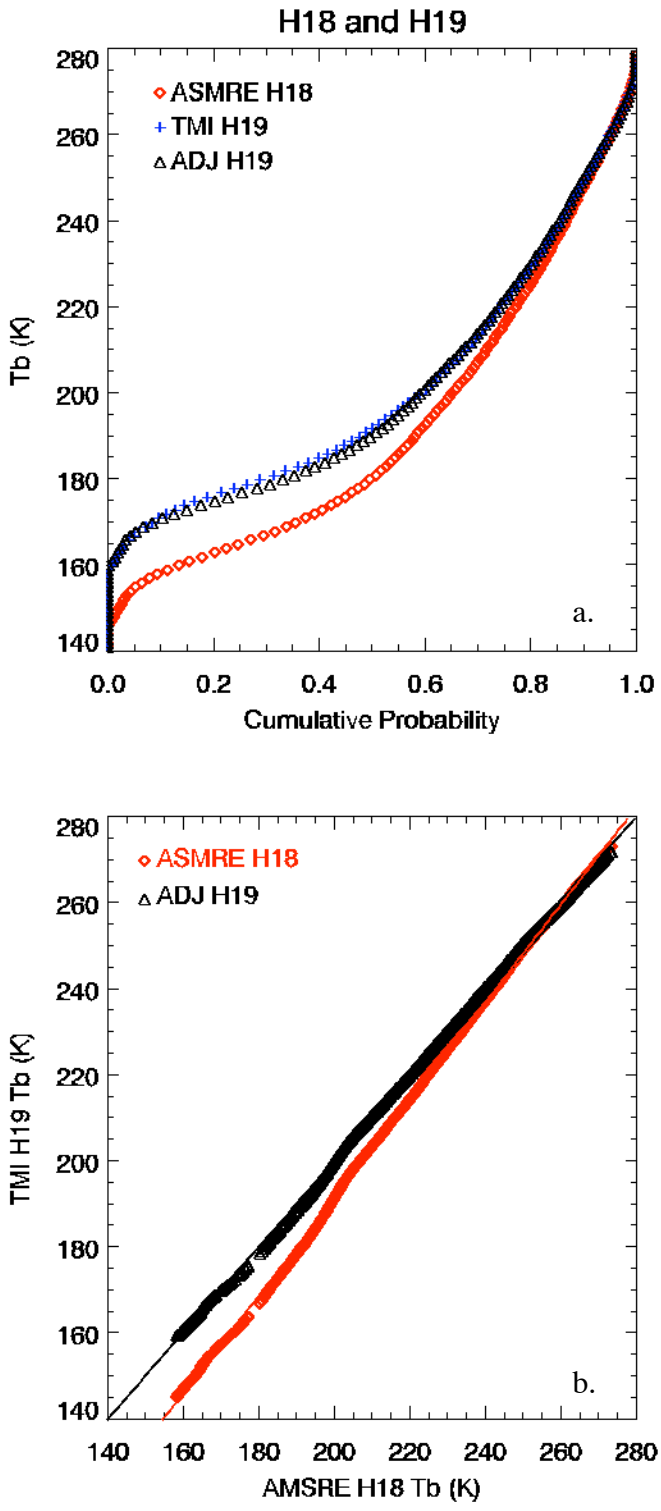

Figure 1. Cumulative distribution functions of AMSR-E H18 and TMI H19 brightness temperatures from the 10-overpass training sample (a). AMSR-E and TMI T_b pairs along lines of equal cumulative probability plotted as a function of each other (b, red points). Results for adjusted H19, using Eq. 1, data are shown for comparison in both plots (black triangles).

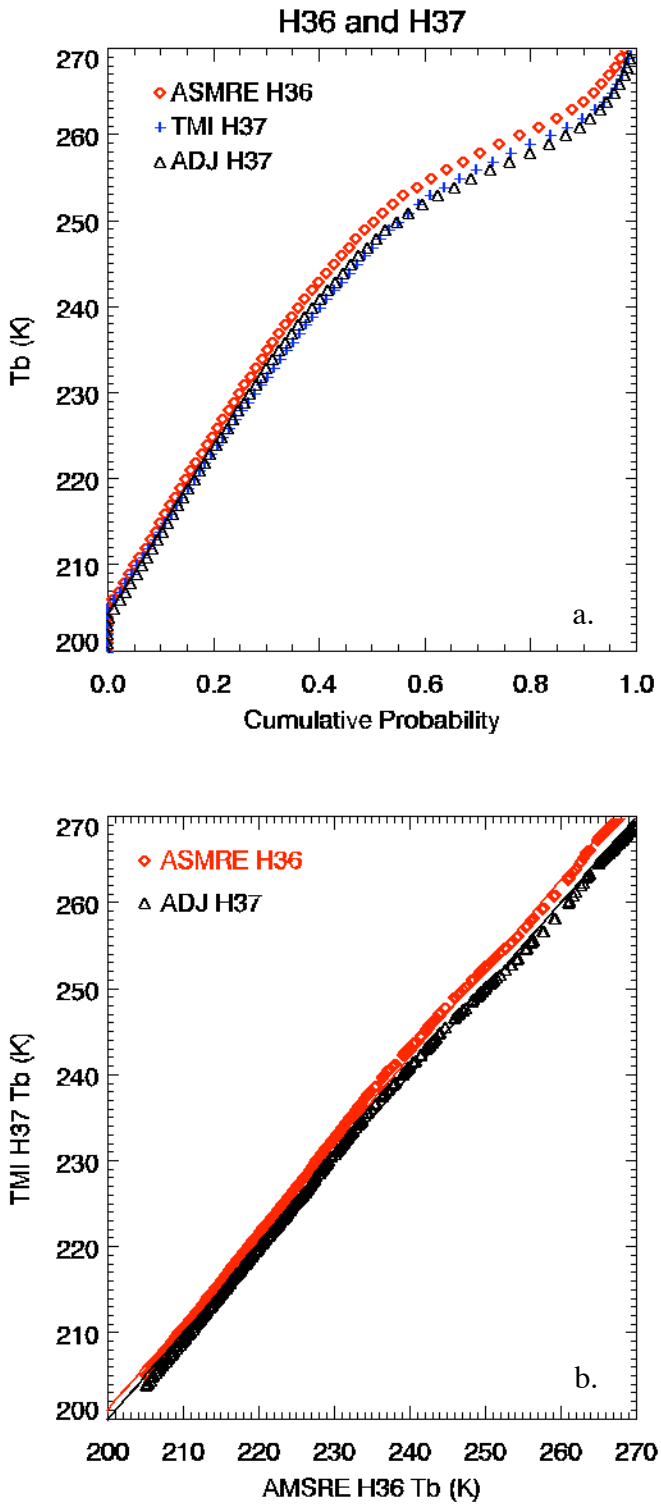

Figure 2. Same as Figure 1, but for AMSR-E H36, TMI H37 and adjusted H37 T_b (Eq. 2). Data below 205 K are not shown.

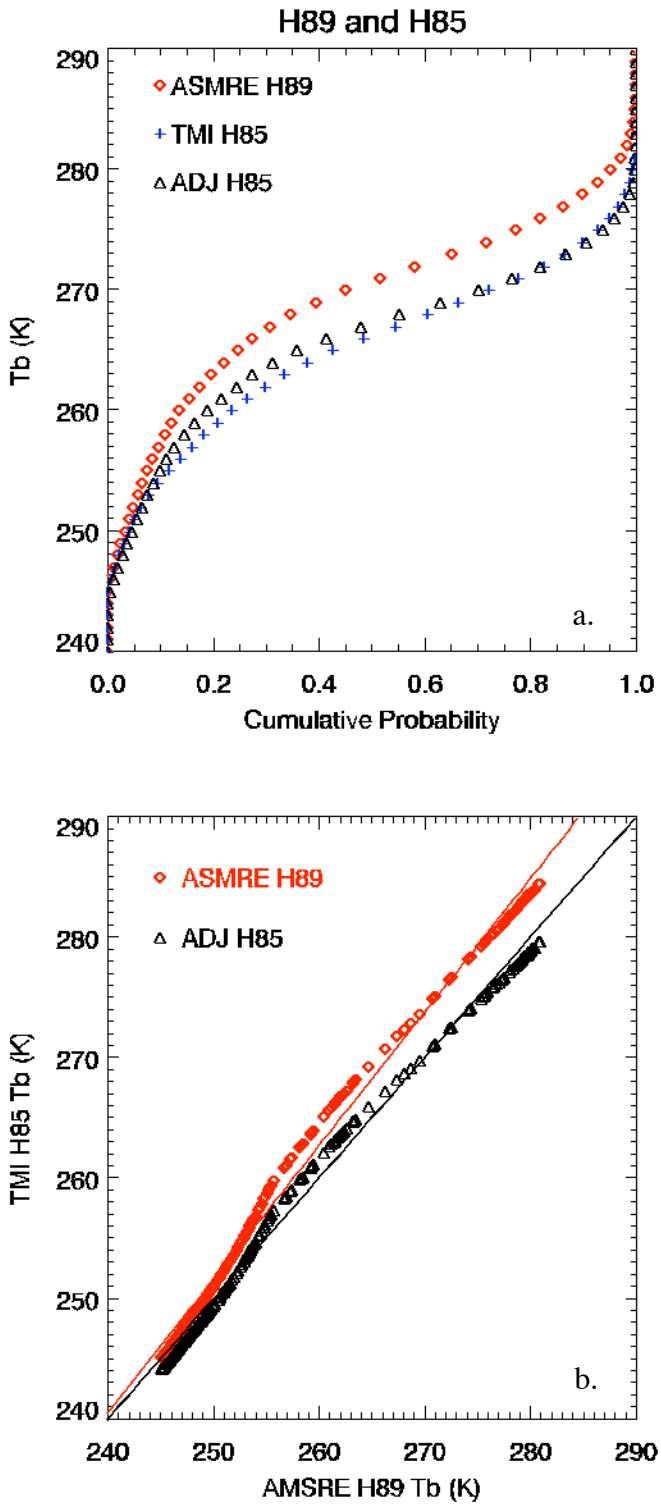

Figure 3. Same as Figure 1, but for AMSR-E H89, TMI H85, and adjusted H85 T_b (Eq. 3). Note the non-linearity in the difference between 250 and 260 K. This prevents the linear adjustment from performing as well as it does for H19 and H37 adjustments. Data below 245 K are not shown.

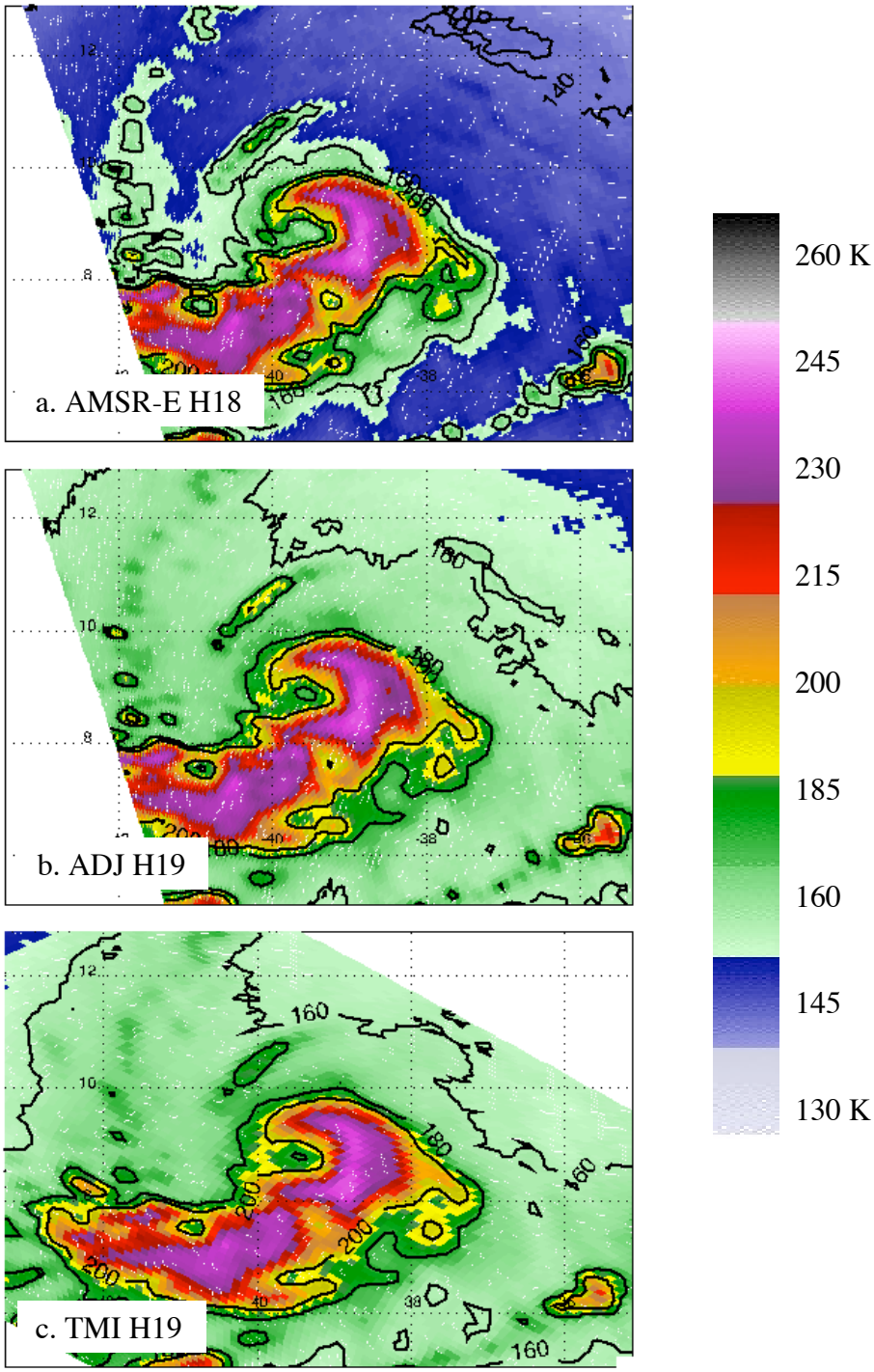

Figure 4. AMSR-E and TMI overpasses of Hurricane Ivan at 1543 and 1537 UTC 4 September 2004 centered on the interpolated best track location at these times. Raw AMSR-E H18 (a), adjusted AMSR-E H19 (b), and TMI H19 (c) are shown with contours at 140, 160, 180, and 200 K overplotted. Note the similarity in the 160 K contour between the adjusted AMSR-E H19 and TMI H19 and how both are ~15 K warmer than H18 in low precipitation regions.

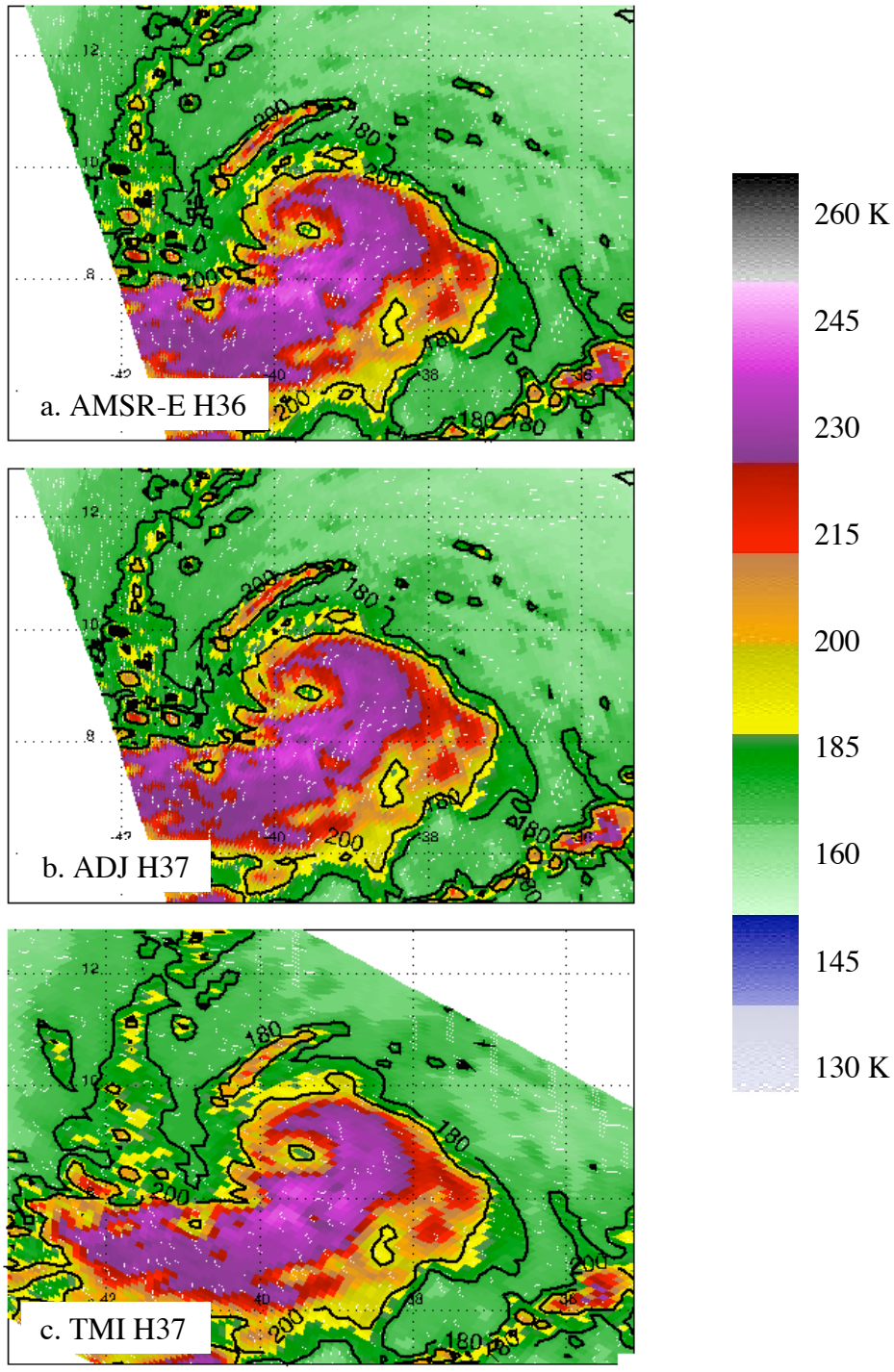

Figure 5. Same as Figure 4, but for raw AMSR-E H36 (a), adjusted AMSR-E H37 (b), and TMI H37 (c) data. Little difference is apparent between raw and adjusted data for this frequency.

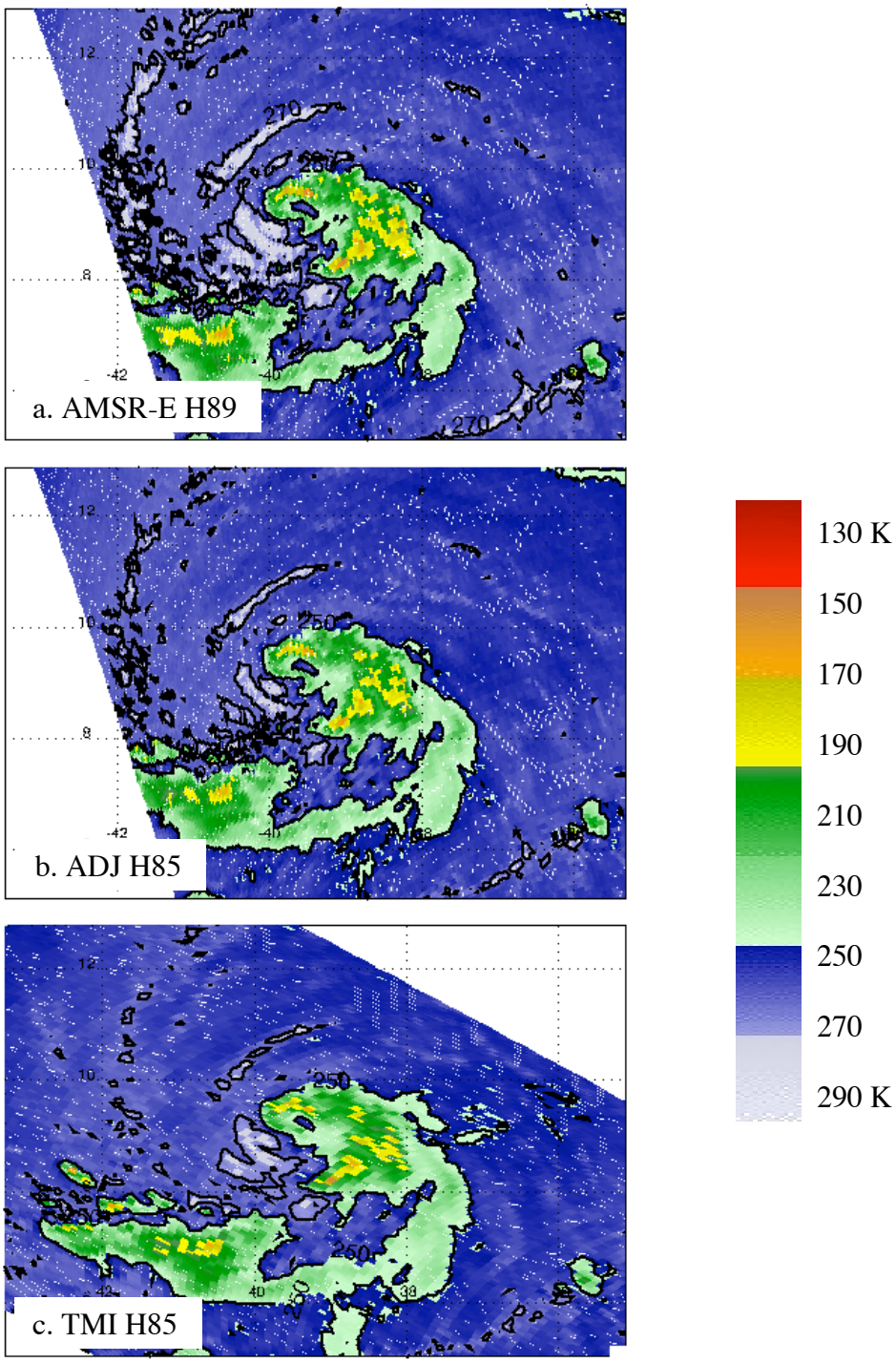

Figure 6. Same as Figure 4, but for raw AMSR-E H89 (a), adjusted AMSR-E H85 (b), and TMI H85 (c) data. 250 and 270 K contours are overplotted. Note the decrease in area of H89 > 270 K when adjusted to H85, which better matches the TMI reference. Regions of strong convection and ice scattering (H89 < 250 K) are not affected by the adjustment.